

A Complex Structural Horn Antenna for Partial Discharge Detection

Abstract. This paper presents a small complex structural Horn antenna sensor on which certain effective structures such as dielectric filled horn, wedge-shaped substrate, and backing cavity are utilized. Model calculation and experimental data show that the antenna possesses a good radiating performance and multi-band property in UHF band.

Streszczenie Opracowanie przedstawia kompletny strukturalny, małych rozmiarów czujnik antenowy horn. Wykorzystano w nim pewne efektywne struktury takie jak: wypełnienie dielektryczne horna, podłoże klinowe i wnękę odbiciową. Obliczenia modelu i dane doświadczalne wykazują, że jest to wielopasmowa antena w zakresie UHF, z dobrymi własnościami promieniowania. **Kompleksowa strukturalna antena Horna do detekcji wylądowań niezupelnych**

Keywords: dielectric filled, microstrip antenna, TEM horn antenna.

Słowa kluczowe: wypełnienie dielektryczne, technika mikropaskowa, antena Horna TEM (poprzecznej fali magnetycznej)

Introduction

Gas insulation substation (GIS) has been increasingly applied in power systems because of its small size, high reliability, and other advantages. However, GIS faults may cause accident enlargement, which can lead to a huge economic loss. Moreover, GIS requires a long maintenance time, thereby affecting a large area of power supply and causing serious consequences. Investigations from the Conference International des Grands Reseaux Electriques indicate that various insulation problems are the main reasons for GIS failure [1]. Information on insulation states can be characterized by partial discharge (PD) signals. The ultrahigh frequency (UHF) method tests electromagnetic (EM) wave signals (300 MHz to 3000 MHz) excited by PD in space, to avoid interference signals from both electrical system and outside. Testing UHF signals cannot only detect the presence of GIS defects, but also estimate the insulation faults and its severity.

Sensors are of two types. Inner sensors possess high sensitivity and strong anti-interference ability [2], but are impossible to install in a GIS already in operation. In comparison, outer sensors or antennas have little influence on the GIS internal electric field and can be easily installed, as such they are more conducive to on-site practice. Commonly used external UHF antennas for PD detection have a low center frequency that cannot simultaneously satisfy both bandwidth and gain requirements. This characteristic is a disadvantage when receiving high-order mode waves, and thus PD cannot be entirely detected. For this reason, the present paper developed a wide-band, small volume, and cavity-backed TEM horn antenna aimed at UHF detection for GIS PD. The microwave simulation and tests using GIS defect imitation shows that the antenna possesses good high frequency performance and suitability for online monitoring and defect identification of GIS.

The Propagation and leakage of EM waves in GIS

A PD occurrence in GIS generates a steep current pulse which, despite a rise-time of only a few nanoseconds, can excite EM waves with several GHz of frequency. The UHF technique measures these EM waves for the early detection of equipment insulation faults.

Leakage occurs when the EM wave travels across the waveguide gaps, which are regarded as slot antennas (Figure 1), and its radiation characteristic is determined by the gap structure. The radiation lobe can be distinguished clearly in this figure. As a transmitting antenna, the slot antenna obtains energy from the waveguide, which, in turn radiates energy back into space. This antenna is adopted

with the outlay sensor installed at the GIS gaps to intercept part of the leaky radiation.

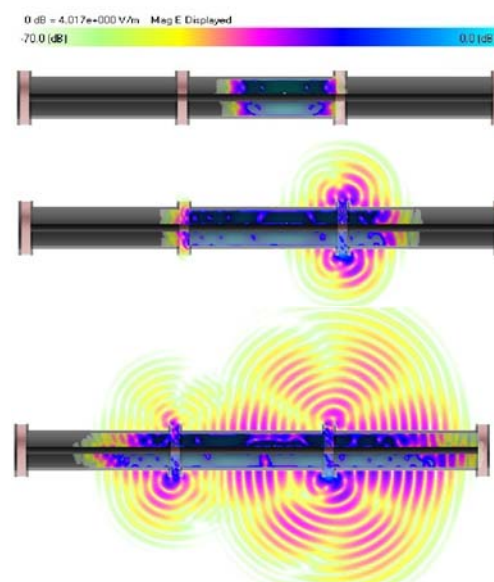


Fig. 1. Leakage progress of EM waves excited by the PD in GIS

The UHF signals which caused by PD travel through the waveguide as TEM, TE, and TM waves inside the GIS. Nondispersive TEM wave can spread in GIS at any different frequency. But TE and TM waves have cut-off frequencies. The wave travels through the waveguide with size $a < r < b$. Among all TE and TM waves, TE_{11} has the lowest cut-off frequency as follows:

$$(1) \quad f_c(TE_{11}) = \frac{c}{\pi(a+b)}$$

where: f_c – cut-off frequency, c – speed of light, a, b – the radius of the conductor and waveguide cavity, respectively.

Considering 500 kV GIS as an example, $a=0.089$ m and $b=0.254$ m, thus $f_c(TE_{11})=278$ MHz. In other words, longitudinal wave propagation will occur only when the PD signal frequency is higher than 278 MHz. For those devices of lower voltage class, cut-off frequency could be even higher correspondingly.

Only TEM wave propagation exists in the area below the cut-off frequency of the TE_{11} wave. There is no cut-off frequency because $f_c(TEM)=0$, $\lambda_c(TEM)=\infty$, and any frequency can satisfy the propagation requirement. The frequency response curve has some wave ripples because

new waves travel at higher frequencies and when above cut-off frequencies of each mode it ascends quickly and periodically [3]. In practice, frequency resonance might cause resonance ranges nearby the cut-off frequencies because of the wave reflection or refraction in the chamber.

The frequency of PD signals caused by tip defects in GIS can reach beyond 1 GHz. The pulse of corona discharge in the air and its rise time can last for a relatively long period. Generally, corona discharges appear at frequencies below 150 MHz, with a quick attenuation when its frequency increases. Thus, PD can be detected by monitoring excited EM waves, especially those of high frequency (300 MHz to 3000 MHz). Thus, interferences when using conventional electrical testing methods can be avoided, such as corona discharge in electrical power system, to increase the signal-to-noise ratio of PD detection.

The Optimization of horn antenna

The horn antenna can be considered as an opened waveguide, which has a high degree of directionality. For many years, TEM horn antennas have been widely used to radiate and receive pulse signals as a kind of ultra-wide band high power antenna, with optimized performance through basic structure modifications such as changing the shape of plates and adding load impedance.

When the basic form of a TEM horn matches a $50\ \Omega$ coaxial cable, the feed point should be located at the head of the parallel waveguide. However, if it is an optimized horn, the new feed point matching with the horn design should be re-found under these circumstances.

Foreign scholars studied the characteristics of the dielectric filled horn as a special form of loading [4]. The horn section between the parallel waveguide and the horn aperture is constructed with a tapered shape, approximating to an exponential rate, to minimize the reflection of the waveguide traveling wave and to decrease the antenna standing wave ratio. This method can likewise reduce side-lobe level.

Using a dielectric filled antenna enables the reception of EM waves of shorter wavelengths. The EM waves are transmitted through the horn when $\lambda \leq \lambda_c$ (cut-off wavelength). Therefore, the dielectric filled antenna can receive more high-order mode signals, allowing received EM signals to maintain good bandwidth and gain despite having a small antenna size.

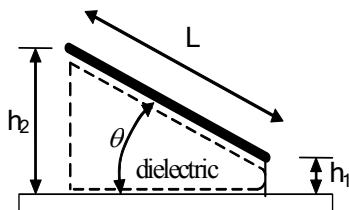


Fig.2. Wedge-shaped dielectric microstrip structure

Ordinary microstrip patch antennas have a narrow bandwidth, and the distance between patch and ground plane is far shorter than the operating wavelength, so EM propagation can be approximately considered as bound in this space. Increasing the distance to half wavelength or longer, the EM waves will no longer be confined to the dielectric material, but will radiate or receive their energy from the patch edge, which forms a quasi-TEM antenna [5]. Microstrip antennas can be equivalent to the parallel resonance circuit with high quality factor, so proper bandwidth can be obtained by virtually redesigning the antenna resonance. This can be achieved by increasing the thickness of the dielectric material or using a special-

shaped dielectric substrate [6,7]. Stepped structure and wedge shape are usually adopted to create special-shaped substrates, increasing the substrate thickness to expand the bandwidth. Moreover, to feed at a thinner edge, this shape can shorten the probe length, reducing the effect of inductive reactance on antenna efficiency. Figure 2 shows the wedge-shaped dielectric structure.

The center frequency of the wedge-shaped dielectric microstrip antenna is:

$$(2) \quad f_c = \alpha \frac{c}{2L \cos \theta \sqrt{\epsilon_r}}$$

$$\theta = \sin^{-1} \left(\frac{h_1 - h_2}{L} \right), \quad \alpha - \text{an extra factor related to the}$$

where: electric field near the edge.

In the current paper, the antenna design follows a multistage microstrip structure aiming to broaden the band. Each patch section has a different slope coefficient.

The antenna positioned in the cavity forms the back cavity structure, and performs better in terms of bandwidth and radiation efficiency compared with antennas without back cavity. The depth of back cavity loaded antenna is about one quarter wavelength of the center frequency wave. Materials absorbing EM waves fill the cavity, which can lead to loss of radiation power, gain reduction, and increased antenna weight.

Characteristics of TEM horn antenna with composite structures

In this paper, the antenna has a semi-closed integral structure. Apart from the direction to which the horn aperture points, the antenna is covered with a metal shell in all other directions, filling dielectric in the back cavity, and fed by a coaxial line. Loaded dielectric in the horn has higher dielectric coefficient than that in the microstrip structure. Thus, the whole antenna can be seen as a dielectric loaded TEM horn antenna with back cavity.

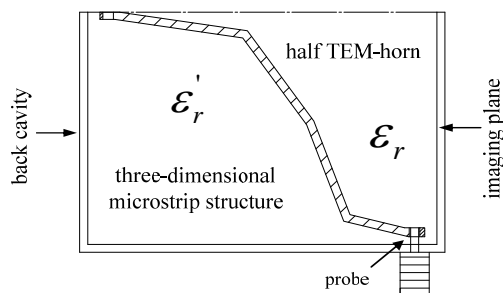


Fig.3. Configuration of the antenna

The design differs from ordinary air microstrip antenna owing to the metal shell. Half the TEM horn section is loaded with a dielectric material with about 6–7 permittivity ϵ_r , and the three-dimensional (3-D) section of the microstrip structure is loaded by a dielectric material with permittivity $\epsilon_r' = 2$. With the composite structure combining stepped structure with wedge shape, the antenna will have a multi-band property. The 3-D microstrip and cavity shell forms a quasi-TEM horn, which can still maintain good radiation characteristics in high frequency; thus, the antenna can work in a wide band.

Simulation results show that the antenna center frequency is about 930 MHz. This result is related to the idealized and approximate process used to deal with the simulation model and the variation of antenna flare angle.

Simulation results show that the antenna center frequency is about 930 MHz. This result is related to the

idealized and approximate process used to deal with the simulation model and the variation of antenna flare angle.

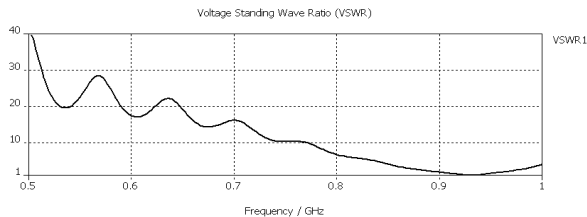


Fig.4. VSWR characteristic with a frequency 0.5–1 GHz

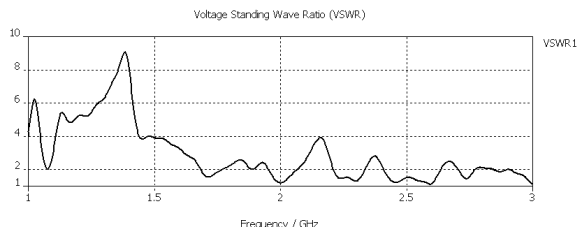


Fig.5. VSWR characteristic with a frequency 1–3 GHz

The antenna status approaches full-wave resonance when nearing 930 MHz, which means reactance is close to zero and the impedance values for pure resistance at the feeding point because voltage and point current are in the same phase. Figure 4 shows that the standing-wave ratio is no more than 2:1 in the band between 880 and 980 MHz, where additional loss can be neglected and the antenna can be considered as completely matched. Figure 5 clearly shows that a $4/2\lambda$ resonance exists. The antenna also shows acceptable standing-wave ratio performance in the range nearing 1.8 GHz.

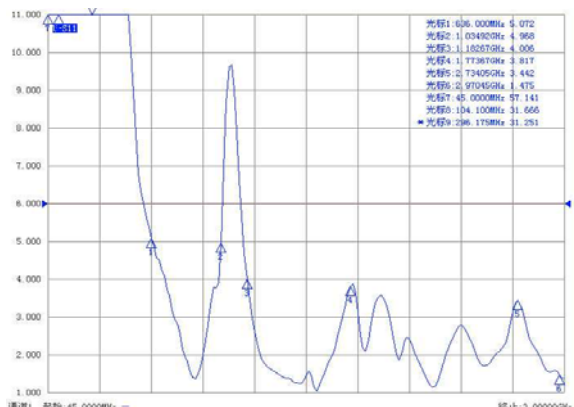


Fig.6. Measured VSWR characteristic of the antenna

In many cases, the value of antenna impedance is unknown, but the measured voltage standing-wave ratio (VSWR) can serve as a substitute. Thus, the module value of reflection coefficient can be calculated from VSWR. Figure 6 shows the measured standing-wave ratio in the range of 45 MHz to 3000 MHz. The antenna has perfect standing-wave ratio within 780–900 MHz, 1.25–1.65 GHz, and 2.15–2.3 GHz, but imperfect ratio below 600 MHz. Generally, the less reflective bands and standing-wave ratio curve tendency are consistent with simulation results.

Antenna gain and pattern

Simulation of radiation patterns from 1 GHz to 3 GHz show that, along with increasing frequency, far-field radiation performance is enhanced and realized gain can then dramatically increase. If antenna radiation frequency rises from 1 GHz to 2.5 GHz, the realized gain would increase from 0.316 dB to 5.07 dB. Although the gain slightly declines when frequency increases to 3 GHz,

requirements for receiving EM signals can still be met with a 3.97 dB gain. As frequency increases, the antenna directionality gradually worsens and the backward lobe distorts. In particular, when frequency reaches 3 GHz, the gain will decrease and the main lobe will divide into two parts. This effect may be caused by the ability of the antenna to receive and radiate higher wave modes at this frequency. Table 1 shows the measured gain.

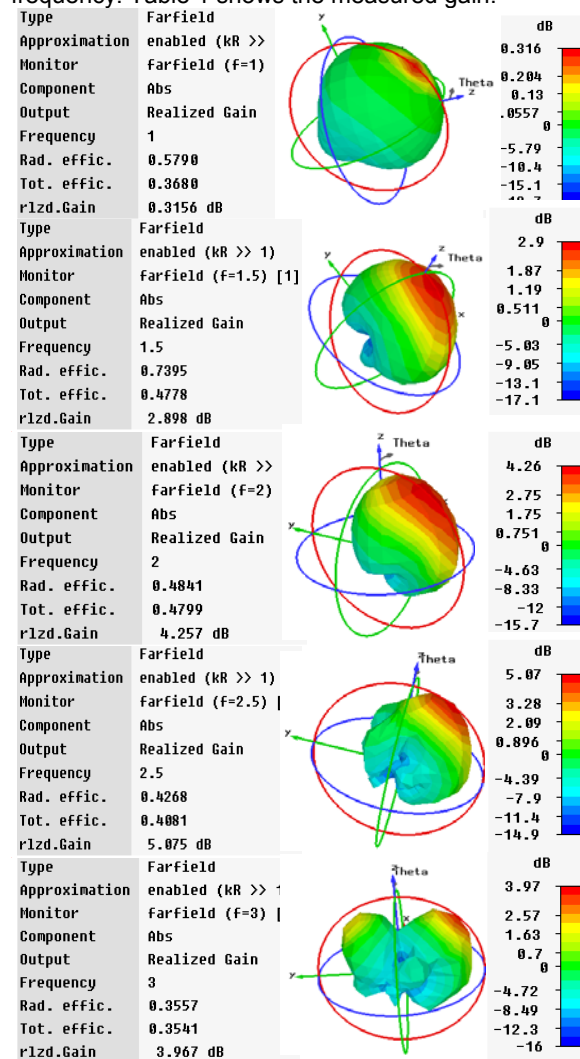


Fig.7. Display of 3-D far-field realized gain pattern

Table 1. Testing record of gain

500 MHz	800 MHz	1 GHz
-12.6dB	-1.4dB	1.3 dB

Figure 8 shows measured gain pattern using the logarithmic coordinate system. The radii of the concentric circles represent the signal voltage logarithm. This coordinate increases the significant level of the side-lobe, reflecting the omnidirectional patterns of the antenna.

In the gain pattern, half power (-3 dB) points can be seen at about 45° and 135°, which means the half power beam width is 90°. Directional difference in all degrees is less than 15 dB. Within 1 GHz frequency, directionality will gradually enhance along with increasing frequency.

The measurements of the antenna

In this experiment, the horn antenna was used to detect artificial GIS defects in the device filled with 0.3 MPa SF₆ gas. Signal waveforms were recorded with a high-speed digital oscilloscope. Furthermore, the current sensing signal received by Rogowski coil was compared for reference.

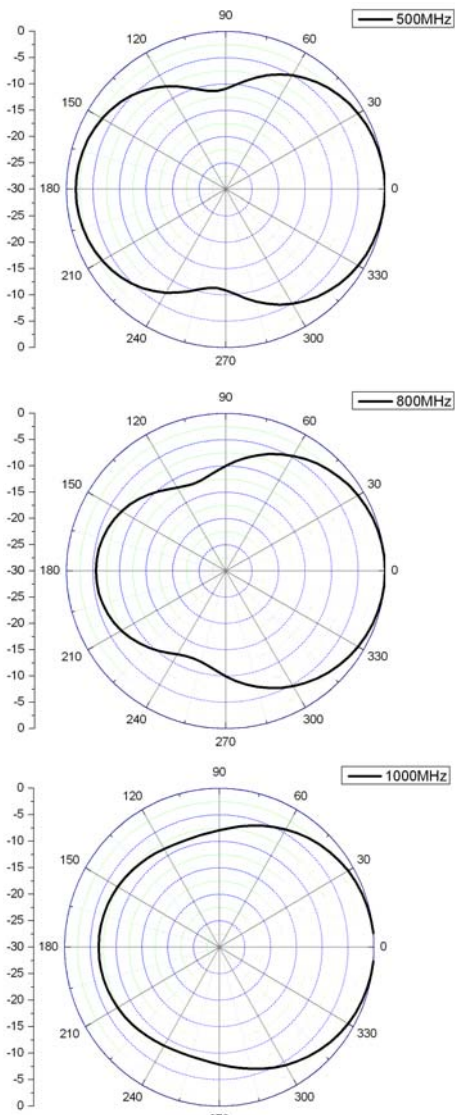


Fig.8. Antenna gain pattern

Needle-plate discharge was used to simulate PD defects. At discharge inception voltage, digitizing voltage signals on the feeder were collected with 5 GS/s sample rate, using both Rogowski coil and horn antenna for synchronous detection. The small horn antenna obtained signals with lower amplitude, but could detect distinct PD signals, satisfying the need for PD detection with high sensitivity.

The human body effect may adversely affect the sensitivity of the small antenna. When the current direction on the antenna is parallel to a human body, which can be considered as a semi-infinite plane reflector of a certain coefficient, the mirror effect generates a current toward the opposite direction, reducing the electric field and increasing the magnetic field. When the small antenna was placed on the ground linked metal or on the surface of GIS cavity, the antenna E-plane should also be perpendicular to the metal surface to obtain the maximum signal amplitude.

A 5 kV ac high voltage was applied to the defect imitation, simultaneously using both microstrip patch antenna (390 MHz center frequency, 25.6% relative bandwidth, 5.38 dB highest realized gain) and dielectric filled horn antenna to receive EM signals radiated from PD. Figure 10 shows that the first waveform curve with 22 mV maximum value represents the signal measured by microstrip antenna, whereas the second waveform curve

with 31 mV amplitude describes the signal measured by the small horn antenna.

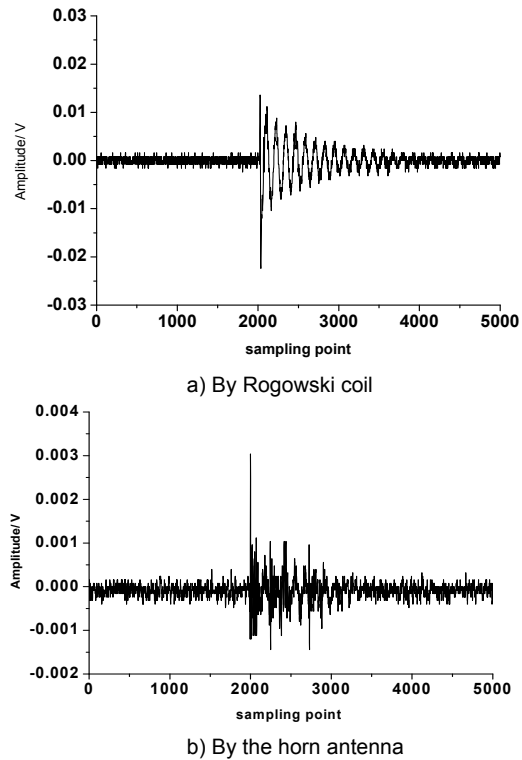


Fig.9. Experiment detected PD signals

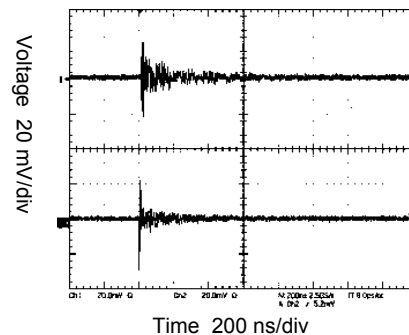


Fig.10. Measured waveforms of UHF signals

In contrast to the microstrip antenna, the horn antenna has a smaller volume and lower gain, but a wider bandwidth. The proposed antenna can receive UHF signals energy from a wider band, reflecting less EM energy and having higher signal attenuation, yet receiving UHF signals with higher amplitude.

Conclusions

Antenna radiation properties were detected through theoretical analysis and simulation on a small quasi-TEM horn antenna. In contrast to the effect of microstrip antenna laboratory measurements, the conclusions can be summarized into the following:

a) The use of TEM horn structure can broaden the antenna bandwidth and maintain good reception performance when in the frequency of 1 GHz and above. The antenna can also receive intact EM signals of PD.

b) Certain effective structures such as dielectric filled horn, wedge-shaped substrate, and backing cavity can be utilized during the antenna design process to enable miniaturization as well as optimize standing-wave ratio characteristics. The latter presents a frequency characteristic of the multiband microstrip antenna due to the adoption of multistage wedge-shaped microstrip structure.

c) Antenna gain tends to increase with antenna frequency within the frequency spectrum of UHF band. Antenna directivity is nearly omnidirectional, and antenna gain meets the requirement of a small receiving antenna. Moreover, compared with normal microstrip patch antennas, the response wave amplitude is higher when receiving PD signals.

REFERENCES

- [1] Gilles Bazannery, Recent Developments in Insulation Monitoring Systems of GISs, *International Electric Power For China*, 6 (2002), No. 4, 41-43
- [2] Dong-suk Kim, Chul-min Hwang, Young-noh Kim, Development of an intelligent spacer built into the internal-type UHF partial discharge sensor, *2008 IEEE International Symposium on Electrical Insulation. Vancouver, Canada: ISEI 2008*, 396-399
- [3] M.D.Judd, O.Farish, B.F.Hampton, Modeling Partial Discharge Excitation of UHF Signals in Wavepde Structures using Green's Functions, *IEE Proceedings, Science, Measurement and Technology*, 143 (1996), No. 1, 63-70
- [4] Y.Huang, M.Nakhkash and J.T.Zhang, A Dielectric Material Loaded TEM Horn Antenna, *Twelfth International Conference on Antennas and Propagation. Exeter, UK: IEEE*, 2 (2003), 489-492
- [5] Feng-Wei Yao, Shun-Shi Zhong, Xian-Ling Liang, Ultra-broadband patch antenna using a wedge-shaped air substrate, *Microwave Conference Proceedings, 2005. Asia-Pacific Conference Proceedings. Suzhou, China: APMC*, 4 (2005), 2698-2700
- [6] Young-Min Jo, Broad band patch antennas using a wedge-shaped air dielectric substrate, *Antennas and Propagation Society International Symposium*, 2 (1999), 932-935
- [7] Debatosh Guha, Sudipta Chattopadhyay, Jawad Y. Siddiqui, Estimation of Gain Enhancement Replacing PTFE by Air Substrate in a Microstrip Patch Antenna, *IEEE Antennas and Propagation Magazine*, 52 (2010), No. 3, 92-95

Authors: prof. dr Xiao-xing ZHANG, State Key Laboratory of Power Transmission Equipment & System Security and New Technology, Chongqing University, Chongqing 400044, China, E-mail: zhxx@cqu.edu.cn; Yang CHEN, Guangdong Electric Power Design Institute, Guangzhou 510663, Guangdong Province, China, E-mail: shenyangcdqz@163.com.